■ Scientific Justification

This proposal aims to infer the physical properties of the gas surrounding two luminous QSOs at z=6.6 for which bright and extended Lyα nebulae have already been detected. These nebulae are potential tracers of the large cool gas reservoirs that are able to sustain the rapid growth in both stellar and black hole mass of the first QSOs. From the detection of the Lyα line alone, however, one can not infer the total mass of gas, nor discern which powering mechanism is responsible for the observed luminosity. Here we propose to carry out sensitive NIRSpec IFU observations of the Hα emission line (and of other species) aimed at lifting these degeneracies, thus setting stringent physical constraints on the gaseous environment of the first massive galaxies. With this study, we will link the growth of the tremendously star forming host galaxies of the first massive black holes with the accretion of pristine material from the intergalactic medium when the Universe is <1 Gyr old.

The Dawn of Galaxy Formation – A prime objective of observational astrophysics is to peer deep into the young Universe and study how the first stars, galaxies, and black holes formed. *JWST* is already revolutionizing this field, providing an unprecedented view of the first *normal* galaxies at z>6 (e.g., Trump et al. 2022, Curti et al. 2022, Fujimoto et al. 2023). On the other hand, while the number of known z>6 QSOs is steadily increasing (see Fan et al. 2022 for a review), there are still several open challenges to our understanding of the formation and evolution of the most massive systems in the young Universe. Indeed, although the Universe is less than 1 Gyr old and the bulk of galaxy formation has yet to occur, z>6 QSOs appear as already evolved systems, with Milky-Way like Fe/α abundances (as derived from the broad line region emission, Schindler et al. 2020), and with black holes of masses $\sim 10^9\,\mathrm{M}_\odot$ (Farina et al. 2022) hosted by galaxies with $M_\star \gtrsim 10^{10.5}\,\mathrm{M}_\odot$ (i.e., among the highest stellar mass galaxies known at $z\sim6$, see Ding et al. 2022 for early *JWST* results). Such a rapid growth is puzzling: the mass increment timescale for a black hole accreting at the Eddington limit is only 45 Myr (Volonteri & Rees 2005), making the Universe only $\sim$ 20 e-folding times old at $z\sim6$. Cosmological hydrodynamical simulations (Sijacki et al. 2009; Costa et al. 2022, Fig. 1) and analytical arguments (Volonteri & Rees 2006) require that, to grow these massive systems in such a short time, the first QSOs must reside within massive halos, where intense star formation episodes are most likely to occur. This picture is supported by the direct detection – through observations of the redshifted CO emission lines – of significant reservoirs of molecular gas (with masses of several $10^{10}\,\mathrm{M}_\odot$) in z>6 QSO host galaxies (Venemans et al. 2017). Additionally, observations of high-z QSOs at (sub-)millimeter wavelengths have revealed high far-infrared luminosities ($\mathrm{L_{FIR}}>10^{12}\,\mathrm{L}_\odot$), implying prodigious star formation rates of $\mathrm{SFR} \gg 100\,\mathrm{M}_\odot\,\mathrm{yr}^{-1}$ (Venemans et al. 2020). Such high star formation rates are in agreement with the detection of bright $[\mathrm{C\,II}]_{158\,\mu\mathrm{m}}$ emission that extends to kpc scales (Venemans et al. 2020). To sustain this intense activity, the first QSOs need a continuous replenishment of fresh fuel provided by filamentary streams of $\mathrm{T}=10^4$–10^5 K gas from the intergalactic medium (IGM). When illuminated by the bright QSO radiation, this fundamental ingredient of early galaxy formation can be directly mapped as an extended "fuzz" of fluorescent Lyα emission (Haiman & Rees 2001).

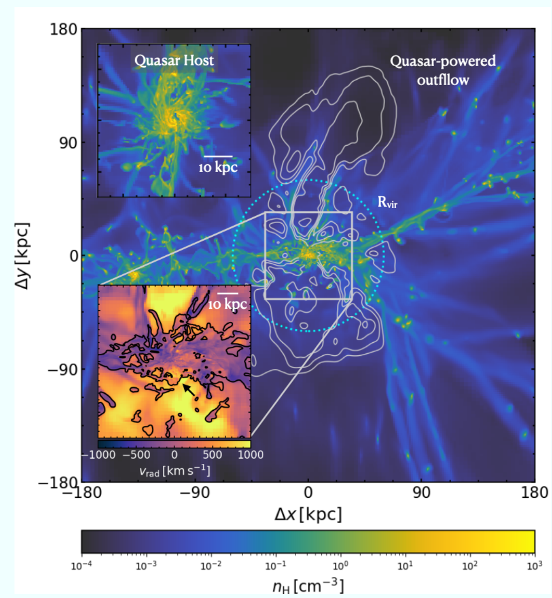

Fig. 1: Cold gas around the first massive black holes. Cosmological radiation-hydrodynamic simulations of the gas density distribution centered on a $z>6$ QSO host galaxy. The host (top left inset) lies in a galaxy overdensity at the intersection of a network of cold gas streams that penetrate the nebulae all the way into the central regions. Velocity contours mark the QSO driven outflow at level of 100, 300, 500 $\mathrm{km\,s^{-1}}$. The bottom left inset plots the gas velocity in the central 70 kpc showing large scale outflows (orange) and inflows (purple) regions. The contours trace dense gas ($n_{\mathrm{H}}>0.1\,\mathrm{cm^{-3}}$). This phase is mostly associated to inflowing gas, and, if it is illuminated by the radiation of the QSO, it will give rise to an extended Lyα nebula (see Costa et al. 2022).

Lyman Alpha Nebulae at Cosmic Dawn – In the last years, *VLT*/MUSE has been intensively exploited to conduct a statistical survey of 31 $z\sim6$ QSOs aimed at detecting the Lyα emission from the gas in the circum-galactic medium (CGM, Farina et al. 2019, Drake et al. 2022). This study provides evidence that large gas reservoirs indeed surround $z\sim6$ QSOs, similar to what was reported around QSOs at $z\sim2$–3 (i.e., almost ~2 Gyr later, Arrigoni-Battaia et al. 2019). Recently, Costa et al. (2022) explored the formation of these Lyα nebulae from a theoretical prospective by post-processing a suite of cosmological, radiation-hydrodynamic simulations with detailed treatment of AGN-feedback of a massive dark matter halo ($M_{\mathrm{DM}}\gtrsim10^{12}\,\mathrm{M_\odot}$) hosting a QSO at $z\sim6$ (Fig. 1). These simulations exposed that the properties of the gas reservoirs are, indeed, the result of many relevant processes in early structure formation (e.g., feeding of pristine gas from the cosmic web-filaments or the metal and gas enrichment due to galaxy scale outflows possibly driven by the black hole activity). In particular, AGN-driven outflows, besides modifying the temperature and density of the gas in the halo, cause a dramatic drop in the H I and dust optical depths in the host galaxy, facilitating the escape of Lyα photons from the galactic nucleus. Thus establishing **a strong causal connection between AGN feedback and Lyα nebulae**. The goal of this proposal is to provide firm observational constraints on these predictions by targeting with NIRSpec IFU the two brightest [with L(Lyα)$>10^{44}\,\mathrm{erg\,s^{-1}}$] and most extended (with projected sizes of $\sim$25 kpc) Lyα nebulae discovered at $z>6$ (Fig. 2). These nebulae could be among **the largest reservoirs of cool gas known in the high-redshift Universe**. However, the same level of emission can be explained by either an exceptionally large total cool gas mass surrounding the first QSOs, or if the gas were organized in a large *mist* of cool, dense gas clouds, which remain unresolved by current cosmological simulations (Cantalupo et al. 2014). Unfortunately, the detection of the Lyα emission alone does not allow to break this degeneracy, and further line diagnostics (such as Hα and [O III]) are necessary to constrain the physical properties of the emitting gas.

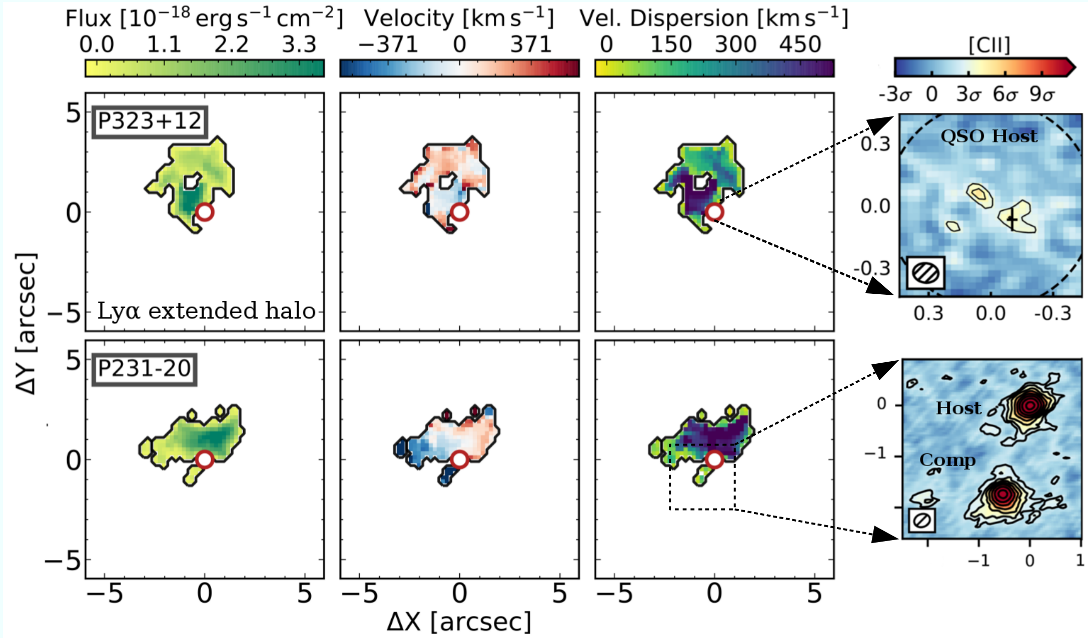

Fig. 2: Large and bright Lyα nebulae around z$\sim$7 QSOs. The two targets of this proposal are the brightest Lyα nebulae known at z>6, with luminosities $\sim 2\times10^{44}$ erg s^{-1} and maximum extents $\gtrsim$20 kpc. As such these are **unique laboratories to dissect QSO's gas reservoirs at the highest redshifts**. In the Figure we show (from the left): integrated flux, velocity field, and velocity dispersion. Intriguingly, the while the nebula around P323+12 shows simple quiescent kinematics, the one associated with P231−21 exhibits hints of coherent rotation. ALMA observations of the [C II]$_{158\,\mu\mathrm{m}}$ emission line (right–most panels) revealed that the nebular emission is intimately linked with the host with velocity separations of <100 km s^{-1}. In addition, these mm-observations revealed a [C II]$_{158\,\mu\mathrm{m}}$ bright companion located $\sim$8 kpc SE from P231−21 (Neeleman et al. 2019).

A Comprehensive View of Galaxy Formation at z$\sim$7 – The two QSOs targeted in this proposal are likely the **signposts of the most active regions of the young Universe**. Indeed, multiwavelength studies of these objects (covering virtually all wavelengths from radio to rest–frame UV) revealed prodigious star formation rates of 200–2000 M$_\odot$ yr^{-1} (Venemans et al. 2019) and massive black holes ($M_{\rm BH}\sim5\times10^9$ M$\odot$) accreting at the Eddington limit (Farina et al. 2022). All these processes quickly consume gas with depletion time scales of $\sim$10–100 Myr. Thus, without a continuous replenishment of cold gas from the IGM, the host galaxies would soon become gas-starved *red-and-dead* objects. The detection of two of the largest and brightest Lyα nebulae known at $z\sim7$ provides circumstantial evidence for massive gas reservoirs able to sustain the intense activity of these objects (Farina et al. 2019). This proposal aims at confirming this scenario by collecting NIRSpec IFU spectroscopy of the extended Hα and [O III] emission associated with these nebulae. With this data we will **(1) precisely quantify the amount of gas present in the proximity of the first black holes, (2) probe its morphology and kinematics, and (3) expose the impact of AGN feedback on the physical status of the CGM**.

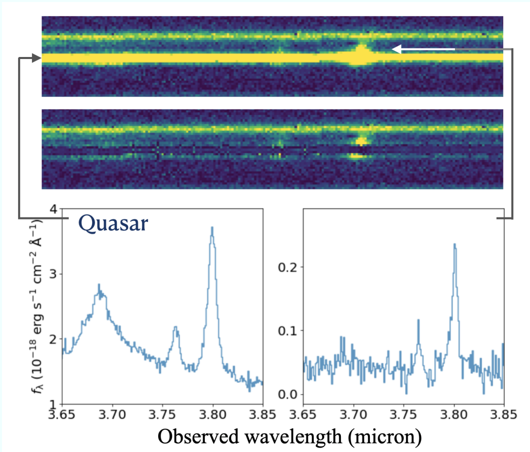

Fig. 3: Extended [O III] emission at z∼7. The 2D WFSS data of the QSO P323+12 (the bright trace in the top-panel image) shows clear extended [O III] emission, in both images before (top row) and after (second row) subtracting the QSO model. The spectrum of the extended emission (bottom-right) is extracted along one line (the white arrow) 2 pixels away from the QSO model. The [O III] lines from the extended region have $\sim$ 200 km s^{-1} offset relative to the QSO's systemic redshift (GO 2078, from private communication).

At z>6.5 the Hα and [O III] emission lines are redshifted to $\lambda \gtrsim 4\,\mu$m, where observations from the ground and even with HST are impossible. *JWST* thus opens a new observational window to probe the presence of low-surface brightness structures even at these redshifts, where theories of the formation and evolution of massive galaxies and black holes can be better constrained (Di Matteo et al. 2012). In detail, the primary goals of this proposal are:

• **Dissecting the Gas Reservoir of the first QSOs** – To date, observations of nebular emission around the first QSOs have been focused on the Lyα line. However, the Hα line is a cleaner probe of ionizing emissivity (Oh 1999). The production rate of Hα photons is 0.45 per recombination, which is comparable to that of Lyα (Hummer & Storey, 1987). Because hydrogen atoms spend such a short time in their n=2 state, the Hα photons do not undergo resonant scattering, and escape from protogalaxies in a single flight. Because an Hα photon is 5/27 times as energetic as Lyα, the intrinsic Hα flux would be expected to be lower. However, the large optical path of Lyα photons due to their random walk out of the gas nebulae makes it virtually impossible to safely attribute the location where it is observed to the location where it was actually produced. Observations of non-resonant lines are therefore necessary to resolve the nature of the extended emission. In particular, **a simultaneous detection of both Hα and Lyα will provide unprecedented information on the status of the gas surrounding the first quasars, allowing a separation of the intrinsic emissivity from radiative transfer effects**. In particular, the ratio between Lyα and Hα fluxes permits to discern among the different mechanisms proposed to power the extended nebular emission: if the ratio is close to the canonical value for *Case B* recombination (∼8.7, Hu et al. 1998), it would indicate that the emission arises from the recombination of hydrogen atoms ionized by the intense radiation of the QSO. Conversely, if a larger ($\gtrsim$12) ratio is observed, the Lyα emission is primarily being produced via *photon-pumping* or scattering of the QSO broadline region (Cantalupo et al. 2014). Finally, if a smaller ratio is observed ($\sim$ 4, as in the case of some Lyα nebulae surrounding z∼2 QSOs, Langen et al. 2023) would imply the presence of dust at CGM scales (Peek et al. 2015), which will produce a reduction of the Lyα emission while the Hα emission will be unaffected. The information on the powering mechanism will allow us to constrain the total mass in cool gas both analytically (Pezzulli & Cantalupo 2019) or via comparison with simulations (Costa et al. 2022).

• **The kinematics of the CGM** – Large scale cosmological hydrodynamic simulations, dedicated to following the earliest phases of z>6 QSO growth suggest that cold accretion onto the first galaxies happens along thin filaments penetrating the halo almost radially (Di Matteo et al. 2017). This kinematic information is expected to be retained by the CGM all the way to the innermost regions, where the baryonic component of the ISM dominates (Cadiou et al. 2022). This prediction can be directly tested by comparing the motions of the Lyα extended emission with those of the Hα and [O III] lines, which are optically thin to the surrounding H I gas, and thus represent the true underlying velocity field of the gas in the CGM. This can be achieved by considering the shift of the Lyα profile relative to e.g., Hα. If it is blueshifted, this implies the presence a higher optical depth of the approaching gas, requiring gas to be accreting. A redshifted Lyα profile, on the other hand, would imply outflowing gas (Yang et al. 2014). In reality, gas accretion models predict different line profile shapes depending on their assumptions. We will thus perform dedicated radiative transfer simulations varying different parameters to compare the relative shapes of Hα and Lyα to predict the detailed geometry and the velocity field of the gas in the CGM.

• **Connect AGN outflow with extended nebular emission** – Given that radiation-hydrodynamic simulations (Costa et al. 2018) predict that warm ($T \sim 10^4$ K) gas dominates the outflow mass budget at kpc scales, the [O III] line has routinely been successfully exploited to trace AGN-driven outflows on scales up to ≈ 20 kpc at cosmic noon (Brusa et al. 2015, Kakkad et al. 2020). The proposed NIRSPec observations will target these forbidden [O III] emission lines at z∼7 at high signal-to-noise. This data will be used to trace the ionized gas properties in the narrow-line region and thus to detect AGN-driven outflows from the [O III] profile. We note that NIRCam slitless data have already been collected for the QSO P323+12 as part of GO 2078 (Fig. 3). This data already show the presence of extend [O III] emission. However, WFSS can not fully resolve the [O III] emission spatially (and its narrow wavelength coverage cannot cover the Hα line). Those exposures are shallower than the one proposed here (due both to shorter exposure and the 3× higher background with respect to NIRSPec). From a spectrally and spatially resolved map of the [O III] lines, we will derive the velocity of the outflowing gas, its geometry, and its mass outflow rate through a multi-component fit of the line profile and exploring a reasonable range of electron densities (Perna et al. 2015). The properties of the detected ionized outflows on kpc scales will be directly linked to the velocity dispersion measured in the targeted Lyα nebulae. We will, thus, test if the powerful outflows can directly (e.g., via the recombination channel) or indirectly (e.g., opening a path of least resistance for the Lyα and UV photons from the central SMBH) contribute to ionizing the CGM further out and generate large-scale Lyα nebulae. Moreover, the detected outflows are also an additional source of ionizing photons ($F_{UV} \propto v^3_{outflow}$, e.g., Allen et al. 2008). These photons are contributing to the observed Lyα nebulae emission via the recombination radiation produced after the photoionization of the cold gas in the CGM. We will thus be able to estimate the contribution of collisional excitation to powering the extended emission, which is predicted to be as high as 100% in case highly inhomogeneous gas ionization and/or a peculiar distribution of the dust in the CGM (Costa et al. 2022).

■ Technical Justification

The goal of our observations is to **fully characterize the presence of ionized gas around the first QSOs independent of its spatial distribution**. Given the large spatial extent and broad velocity range spanned by the two nebulae under consideration (Fig 2), NIRSpec IFU is the **only** instrument available to perform our experiment. The sensitivity required for this study is indeed prohibitive from the ground, even in the light of 30-m class telescopes. We stress that the Hα emission we aim to study is not the central and unresolved broad line emission emerging from material orbiting the central supermassive black hole. Instead, it is the the diffuse Hα emission centered at the systemic redshift of the source (precisely derived from the $[\mathrm{C\,II}]_{158\,\mu\mathrm{m}}$ emission line) which is expected to extend over scales of several kpc from the QSOs (based on Lyα studies). *JWST* has the unique capability of separating the bright central emission of the underlying host from the extended nebula.

Targets – For this proposal we select the two brightest Lyα nebulae known at $z>6$ (Farina et al. 2019, Drake et al. 2022). As such, they are ideal laboratories to explore the physical properties of the gas reservoirs of the first QSOs. The two associated QSOs P323+12 (z=6.588) and P231−20 (z=6.586) are among the brightest sources known at these redshifts (M_{1450}=−27.1 mag) and have thus been subject to extensive multiwavelength campaigns (including *HST* and *JWST* NIRCam, Mazzucchelli et al. 2019, Fig. 3). This observational effort revealed black holes with similar masses ($\sim5\times10^{9}\,\mathrm{M}_\odot$) but dramatically different host-galaxies. ALMA high–spatial resolution observations ($\lesssim0\farcs3$ or $\lesssim1.5$ kpc, Fig. 2) showed that P231−20 is hosted by a highly star forming galaxy ($>2000\,\mathrm{M}_\odot\,\mathrm{yr}^{-1}$) in interaction with a close $[\mathrm{C\,II}]_{158\,\mu\mathrm{m}}$-bright companion. The host of P323+12, instead, is less active with SFR$\sim200\,\mathrm{M}_\odot\,\mathrm{yr}^{-1}$ (Venemans et al. 2020). The Lyα nebulae of these two QSOs have luminosities of L(Lyα)$\sim$10-20$\times10^{43}\,\mathrm{erg\,s}^{-1}$ and scales of $\gtrsim3''$. Intriguingly, the kinematics of the two systems is different. The nebula associated with P323+12 is broad (FWHM$\sim1400\,\mathrm{km\,s}^{-1}$) with no hint of ordered motion. Conversely, the extended emission around P231−20 shows a clear velocity gradient ranging from −200 to +800 $\mathrm{km\,s}^{-1}$ East to West (Fig. 2). Despite targeting only two objects for this study, we are nonetheless exploring a variety of properties of the host galaxy and the nebular emission.

Spectral setup – The only NIRSpec gratings that effectively cover the Hα line, which is of central interest for this project, are G395H/F290LP (with resolution R$\sim$3000, or 100 $\mathrm{km\,s}^{-1}$) and G395M/F290LP (R$\sim$1000 or 300 $\mathrm{km\,s}^{-1}$). In order to preserve the kinematics imprinted in the nebular emission and to spectrally resolve the [O III] outflows, we opt for the G395H/F290LP configuration. In a single shot, this grism covers Hα and [O III] together with several other lines such as Hβ and [N II]. While the emission of the Hβ and [N II] lines from the nebula is expected to be low (the ratio between Hα and Hβ fluxes is $\sim$3), the [O III] lines will have a comparable strength (or even stronger) with respect to Hα (see Fig. 3). These additional diagnostics will provide extra information on the metallicity and ionization status of the nebulae, on the interstellar medium of the host-galaxies and of the close companion of P231−20, and will permit us to infer precise black hole masses based on the Hα and Hβ broad lines (Eilers et al. 2022).

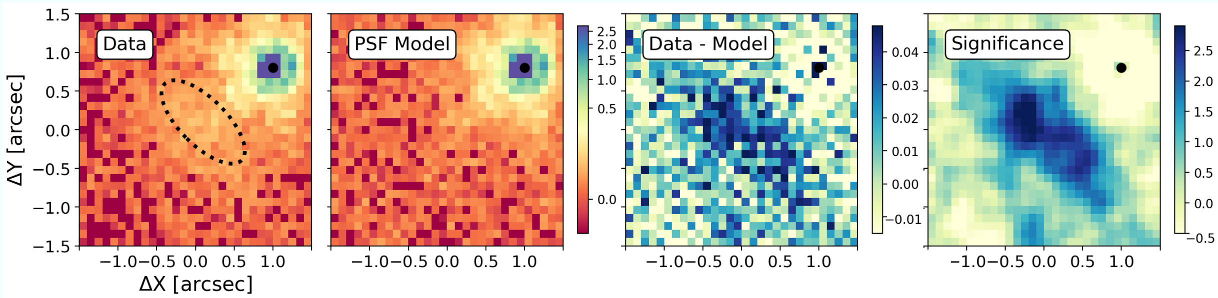

Fig. 4: PSF contamination tests. From left to right: *(i)* ETC simulation of the scene described in the *Observing Strategy*, the contamination of the QSO emission (black dot) is apparent above the extended emission model (highlighted with a black ellipse). The image was obtained by collapsing 10 channels at the expected location of the Hα line. *(ii)* PSF model obtained collapsing the cube in the wings of the QSO broad Hα line. *(iii)* Residual after model subtraction. *(iv)* Smoothed significance map (formally: `SMOOTH[(DATA-MODEL)]/SMOOTH`^{2}`[NOISE]`). With this procedure we were able to detect the full nebula with a S/N$\sim$30. Note this test aims at mimicking the configuration in the sky of the QSO P231$-$20 and the surrounding nebula (see Fig. 5).

Observing Strategy – The goal of the proposed NIRSpec IFU observation is to obtain Hα emission line flux and velocity maps of the extended gas reservoir surrounding two bright QSOs, after the subtraction of the central source resulting from nuclear emission. We stress that, given that Lyα and Hα are tracing the same element, the previous knowledge of the emission level and location of the Lyα nebulae makes this experiment particularly efficient. The total exposure time is estimated by rescaling the total luminosity and the extent of the Lyα emission considering a *Case B* recombination scenario. To estimate the exposure time necessary for a significant detection of the nebular emission, we created mock observations that include the following components:

(1) *QSO emission* – The Selsing et al. (2016) QSO composite was redshifted to z=6.59 and scaled to match the observed J-band magnitude of the QSOs ($J_{\rm AB}$=19.7 mag). The QSO is a point source located at (+1″,+1″) from the center of the the NIRSpec IFU detector.

(2) *Host galaxy emission* – Given the constraints on mass and SFR derived from mm–wavelength observations, we consider the host galaxy as a starburst with stellar mass $\sim6\times10^{10}$ M$_\odot$ shaped as a Sérsic profile with $r_{\rm e}$=1.7 kpc centered at the QSO location.

(3) Hα *nebular emission* – We consider an emission line with FWHM=1000 km s^{-1} and a total luminosity of 4.6×10^{43} erg s^{-1} (a factor 8.7× lower than Lyα). The profile of the nebula is a 2D Gaussian distribution with sigmas of 0.″3 and 0.″7 located at the center of the detector with an inclination of 45°. This configuration reflects the asymmetrical profile observed for the two Lyα nebulae considered in this proposal (Fig. 2, 4).

We consider 6 exposures in a cycling dither pattern and 20 groups per integration. The NRSIRS2 readout mode has been employed to reduce the data rate while efficiently removing cosmic rays. The total observing time will thus be of 2.4 hours per target. The peak of the Hα line will thus be detected at S/N$\sim$6 over an aperture of 1 arcsec^2 and the entire nebula (integrating over the entire spatial and velocity extent) with S/N$\sim$30. This will also allow to detect the peak of the Hα line at S/N$\sim$3 over an aperture of 1 arcsec^2 even if the Lyα to Hα ratio is as low as ~ 4 (see above for details). To estimate the impact of the wings of the QSO emission on our detection limit we tested our PSF extraction algorithm over the datacube simulated by the ETC. The results are shown in Fig. 4: after removing the contribution from the QSO and its host galaxy we were able to extract the nebular emission with a S/N$\sim$5 over a 1 arcsec^2 aperture and the full nebula with a S/N$\sim$25. We stress that, given the nominal spectral resolution of G395H/F290LP we will be able to fully resolve the large scale motion of the gas over several resolution elements at high significance.

Target acquisition – The pointing accuracy of *JWST* is $0\farcs1$, which is sufficient for our science. We thus do not require a target acquisition observation (reducing overheads).

Background – The size of the Lyα nebulae we propose to observe is comparable with the NIRSpec IFU FoV. However, the Lyα emission is highly asymmetrical and the Hα emission, could be not co-spatial with the Lyα one. We thus include an second position to cover the emission of the QSO, of the surrounding host galaxy (with a size $<0\farcs3$ as expected from mm-observations), and of the [O III] outflow detected in NIRCam data (Fig. 3). In this way we will uniformly cover the QSO surrounding, double the exposure time on the central regions, and precisely control the background level from the data without extended emission.

PSF subtraction – The nebulae target of this program are clearly offset from the QSO emission. This makes the need of a perfect PSF subtraction less urgent than in other systems (see Fig. 4). Nevertheless, to maximize the science return of these observations (e.g., revealing stellar light from the host galaxy, exploring the full extent of the Hα nebulae, etc.) we plan to subtract the central point source using PSF decomposition tools currently in development. In general, we will explore both empirical PSF models from the GTO and ERS (Wylezalek et al. 2022) observations, the `WebbPSF` software, and we will develop our own routines to derive the PSF based on spectral regions not contaminated by extended emission.

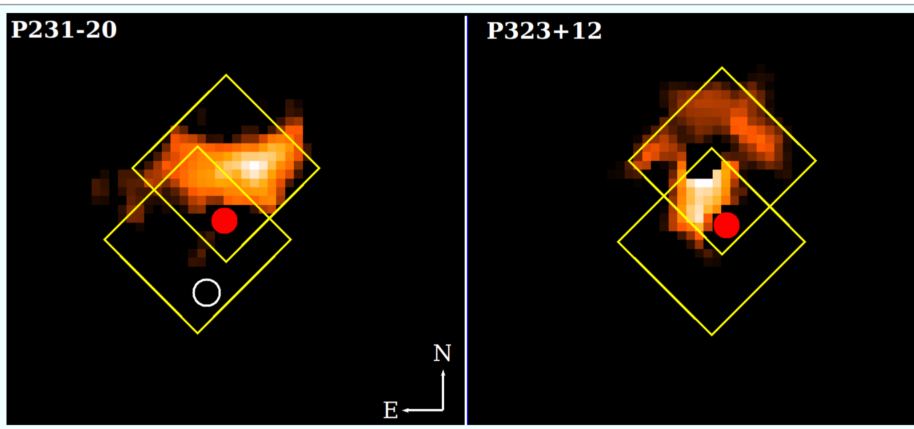

Fig. 5: Observing strategy. The two nebulae fit well within the NIRSpec IFU FoV (yellow squares). During the same visit, a *background* exposure will also be taken, covering the QSO and the host galaxy (red dot) but pointing to a region where no Lyα extended emission has been detected. In the case of P231−20, a rest–frame optical spectrum of the galaxy companion (white circle) will also be collected within the same exposure.

- **Special Requirements (if any)**

- **Justify Coordinated Parallel Observations (if any)**

- **Justify Duplications (if any)**

- **Analysis Plan (AR only)**

References • Arrigoni Battaia et al. 2019, MNRAS, 482, 3162 • Costa, T., Arrigoni Battaia, F., Farina, E. P., et al. 2022, MNRAS, 517, 1767 • Curti, M., D'Eugenio, F., Carniani, S., et al. 2023, MNRAS, 518 • Ding, X., Onoue, M., Silverman, J. D., et al. 2022, arXiv:2211.14329 • Drake, A. B., Neeleman, M., Venemans, B. P., et al. 2022, ApJ, 929, 86. • Haiman & Rees 2001, ApJ, 556, 87 • Eilers, A.-C., Simcoe, R. A., Yue, M., et al. 2022, arXiv:2211.16261 • Fan, X., Bañados, E., & Simcoe, R. A. 2022, arXiv:2212.06907 • Farina, E. P., Schindler, J.-T., Walter, F., et al. 2022, ApJ, 941, 106. • Fujimoto, S., Arrabal Haro, P., Dickinson, M., et al. 2023, arXiv:2301.09482 • Peek, J. E. G., Ménard, B., & Corrales, L. 2015, ApJ, 813, 7 • Pezzulli, G. & Cantalupo, S. 2019, MNRAS, 486, 1489. • Schindler, J.-T., Farina, E. P., Bañados, E., et al. 2020, ApJ, 905, 51 • Trump, J. R., Arrabal Haro, P., Simons, R. C., et al. 2022, arXiv:2207.12388 • Venemans, B. P., et al. 2017, ApJ, 845, 154 • Venemans, B. P., Walter, F., Neeleman, M., et al. 2020, ApJ, 904 • Volonteri & Rees, 2006, ApJ, 650, 669 • Volonteri 2010, A&ARv, 18, 279 • Wylezalek, D., Vayner, A., Rupke, D. S. N., et al. 2022, ApJL, 940, L7.